

DESY 95/057
LMU 07/95
hep-ph/95?????
March 1995

Higgs production in $e^+e^- \rightarrow \ell\ell q\bar{q}$ at LEP and NLC

Dima Bardin^{1,2}, Bernd Leike³ and Tord Riemann¹

¹ DESY – Institut für Hochenergiephysik, Platanenallee 6, D-15738 Zeuthen, Germany

² Bogoliubov Laboratory for Theoretical Physics, JINR, ul. Joliot-Curie 6, RU-141980 Dubna, Moscow Region, Russia

³ Sektion Physik der Ludwig-Maximilians-Universität, Theresienstr. 37, D-80333 München, Germany

Abstract

Predictions for Higgs production with processes of the type $e^+e^- \rightarrow \ell\ell q\bar{q}$ at LEP-2 and the NLC are calculated. Short analytical formulae describe the double differential distribution in the invariant masses of the $\ell\ell$ and $q\bar{q}$ pairs. The total cross section may be got with two numerical integrations. The various Higgs-background interferences vanish either identically or are small. The background contributions depend strongly on cuts applied on the invariant masses.

email: bardindy@cernvm.cern.ch, leike@cernvm.cern.ch, riemann@ifi.de

³ Supported by the German Federal Ministry for Research and Technology under contract No. 05 GM U 93P and EU contract CHRX-CT-92-0004.

1 Introduction

The e^+e^- colliders LEP 2 and NLC (Next Linear Collider) allow to search for a light Higgs boson with the on-shell Higgsstrahlung process of figure 1a and its background,

$$e^+e^- \rightarrow \gamma^* \rightarrow b\bar{b}; \quad (1)$$

where b stands for a heavy fermion ($b; c; \dots$) with sizeable coupling to the Higgs and γ^* for a different one ($\gamma; u; d; s$). Among these final states, $\gamma^* \rightarrow b\bar{b}$ has a very clean experimental signature. In the SM (Standard Model), a light Higgs boson with a mass in the region $60 \text{ GeV} < M_H < 120 \text{ GeV}$ would decay with a rate of about 85%–65% into $b\bar{b}$. Much less frequent are other two fermion ($2f$) final states: $\gamma^* \rightarrow \tau^+\tau^-$, $c\bar{c}$. Above $M_H \sim 120 \text{ GeV}$, different processes become more important; these will not be considered here¹.

Besides the Higgs signal, there are additional contributions from other 4 fermion ($4f$) production processes, which are topologically indistinguishable from Higgs production and will be called background. They proceed via diagrams with an intermediate $Z Z^*/Z$, or γ^* state (figure 1b) or through the diagrams of figure 2. Further background exists if the final state contains an e^+e^- pair or neutrinos. If the two light final state fermions are light quarks, which produce hadronic jets one has to add incoherently also the production of the $b\bar{b}$ pair together with two gluonic jets.

In this letter, we present a complete analytical study of the invariant mass distribution of (1) with the following observable final states:

- (i) $[\gamma^* \rightarrow b\bar{b}]$;
- (ii) $[\gamma^* \rightarrow l\bar{l}], l = e, \mu, \tau; [\gamma^* \rightarrow q\bar{q}];$
- (iii) $[\gamma^* \rightarrow q\bar{q}; b\bar{b}], q \neq b; [\gamma^* \rightarrow q\bar{q}; c\bar{c}], q \neq c.$

The pure background cross section has been studied in [2] and few numerical results for the complete process may be found in [3]. The Monte Carlo approach has been used in [4].

In the next section, we will calculate the on-shell Higgs cross section. In section 3, some numerical results are discussed.

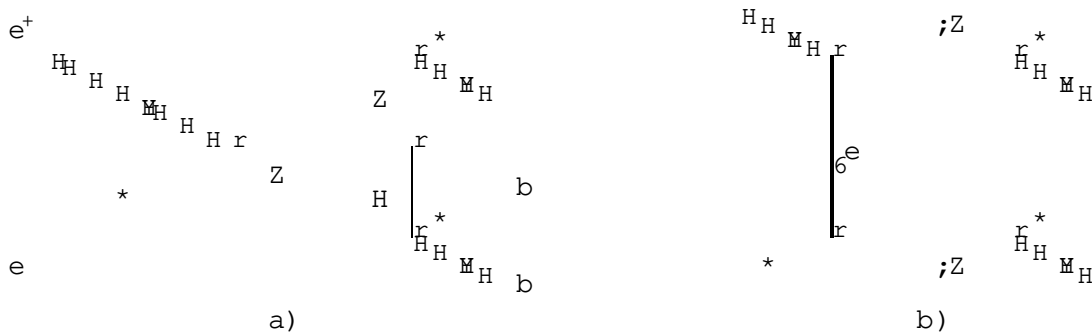


Figure 1: The Feynman diagram for on-shell ZH production (a) and one of the two background diagrams of the crab type (b).

¹ For a review on basics of (mainly on mass shell) Higgs physics we refer to [1] and references therein.



Figure 2: The b-deer diagrams. The l-deers may be obtained by interchanging the leptons with the quarks.

2 The formulae

After integrations over four fermion angles and the production angle of one of the virtual bosons, the following phase space integrals remain to be performed:

$$(s) = \int_{4m_b^2}^Z \frac{p_{\bar{s}}^2}{s} ds_Z \int_{4m_b^2}^Z \frac{p_{\bar{s}}^2}{s} ds_H \frac{p_{\bar{s}}^2}{s} \frac{1}{s_Z} \frac{1}{s_H} \frac{1}{ds_Z ds_H} d^2(s; s_Z; s_H); \quad (2)$$

with the usual definition of the function, $(a; b; c) = a^2 + b^2 + c^2 - 2ab - 2ac - 2bc$, and $(s; s_Z; s_H)$. The s_Z and s_H are the virtualities of the bb and bb pairs, correspondingly. The cross section consists of several pieces:

$$\frac{d^2(s; s_Z; s_H)}{ds_Z ds_H} = H + H_e + H_f + H_b + \text{backgr}; \quad (3)$$

Index H means the squared Higgs signal diagram, while index H_f (with $f = e; b$) denotes the interference of the signal diagram with the crabs (or conversion diagrams) and the e - and b -deers (or annihilation diagrams). The background cross section $\text{backgr} = \sigma_e + \sigma_b + \sigma_{e\bar{e}} + \sigma_{b\bar{b}} + \sigma_{e\bar{e}b\bar{b}}$ is not related to the Higgs boson and has been studied in [2]. Again, index f denotes the square of the sum of f -deers and index $f_1 f_2$ the corresponding interferences. The matrix elements have been squared and integrated over the five angular variables by two independent calculations with use of FORM and CompHEP [5].

The on-shell Higgs signal H reads:

$$\begin{aligned} H &= \frac{d^2 H(s; s_Z; s_H)}{ds_Z ds_H} \\ &= \frac{1}{s} T_H C_{222}(b; s_H; e; s; s_Z) G_{222}(s_H; s; s_Z); \end{aligned} \quad (4)$$

with: T { a color factor, C { a coefficient function containing neutral boson propagators and boson fermion couplings, and G { a kinematic function, which depends only on s and the two virtualities:

$$\begin{aligned} T_H &= N_c(b) N_c(\bar{b}); \\ C_{222}(b; s_H; e; s; s_Z) &= \frac{2}{(6^2)^2} m_b^2 C_H^4 \frac{1}{\mathcal{D}_Z(s)^2 \mathcal{D}_Z(s_Z)^2 \mathcal{D}_H(s_H)^2} \\ &\quad [L(e; Z)L(e; \bar{Z}) + R(e; Z)R(e; \bar{Z})] \end{aligned} \quad (5)$$

$$[L(\bar{f}; Z)L(f; Z) + R(\bar{f}; Z)R(f; Z)]; \quad (6)$$

$$G_{222}(s_H; s; s_Z) = \frac{1}{4}s_H(s + 12ss_Z); \quad (7)$$

The conventions for the left- and right-handed couplings between vector bosons and fermion f are: $L(f;) = R(f;) = (eQ_f)/2$, $L(f; Z) = e(4s_W c_W)(2I_3^f - 2Q_f s_W^2)/4$, $R(f; Z) = e(4s_W c_W)(-2Q_f s_W^2)/4$. Further, $C_H = e(4s_W c_W)$. We use in weak amplitudes $e = 1/(4(2M_W))$, $Q_e = -1$, $I_3^e = \frac{1}{2}$, and $(2M_W) = 1/128.07$ and define $s_W^2 = (2M_W)^2/(2M_W^2 + G_F)$. For photon propagators, $e(1/s_Z)$ is used instead. Color factors are $N_c(f) = 1$ (3) for leptons (quarks). The numerical input for the figures is $G_F = 1.16639 \times 10^{-5} \text{ GeV}^2$, $M_Z = 91.1888 \text{ GeV}$, $M_W = 80.230 \text{ GeV}$, $m_Z = 2.4974 \text{ GeV}$, $m_b = 4.8 \text{ GeV}$, and $D_B(s) = (s - M_B^2 + i\epsilon \bar{s}_B(s))^{-1}$.

Another notion exhibits the on shell limit more explicitly [3]:

$$\Gamma_H = \frac{2G_F M_Z^2 M_W^2}{s s_Z s_H} G_{222}(s_H; s; s_Z) \sum_{f \neq e^+e^-} |s_Z| \Gamma_H \rightarrow b\bar{b}(s_H); \quad (8)$$

where $\Gamma_H \rightarrow b\bar{b}(s) = \frac{1}{s} \Gamma_H \rightarrow b\bar{b}(s) = \frac{1}{s} \frac{M_B^2 + iM_B \Gamma_B(s)}{G_F} \sum_f N_c(f) m_f^2$. For the Higgs width, we use the Born formula $\Gamma_H(s) = \frac{1}{s} G_F = (4/2) \sum_f N_c(f) m_f^2$ in our numerics. In the Higgs mass range considered here this is a sufficiently good approximation. The on shell limit is: $\lim_{s \rightarrow 0} \Gamma_H(s) = (s - M_B^2) \text{BR}(H \rightarrow b\bar{b})$.

The $H \rightarrow b\bar{b}$ interference is:

$$\begin{aligned} \Gamma_{Hb} &= \frac{d^2 \Gamma_{Hb}(s; s_Z; s_H)}{ds_Z ds_H} \\ &= \frac{1}{s} T_H [C_{322}(b; s_H; e; s; s_Z) G_{322}(s_H; s; s_Z) + C_{322}^a(b; s_H; e; s; s_Z) G_{322}^a(s_H; s; s_Z)]; \end{aligned} \quad (9)$$

with the coupling functions

$$\begin{aligned} C_{322}(b; s_H; e; s; s_Z) &= \frac{2}{(6-2)^2} m_b^2 C_H^2 \\ &\times \sum_{V_1, V_2 = Z} \frac{1}{D_Z(s) D_Z(s_Z) D_H(s_H) D_{V_1}(s) D_{V_2}(s_Z)} \\ &[L(e; Z)L(e; V_1) + R(e; Z)R(e; V_1)] \\ &[L(\bar{e}; Z)L(\bar{e}; V_2) + R(\bar{e}; Z)R(\bar{e}; V_2)] \\ &[L(b; V_1)L(b; V_2) + R(b; V_1)R(b; V_2)]; \end{aligned} \quad (10)$$

$$\begin{aligned} C_{322}^a(b; s_H; e; s; s_Z) &= \frac{2}{(6-2)^2} m_b^2 C_H^2 \\ &\times \sum_{V_1, V_2 = Z} \frac{1}{D_Z(s) D_Z(s_Z) D_H(s_H) D_{V_1}(s) D_{V_2}(s_Z)} \\ &[L(e; Z)L(e; V_1) + R(e; Z)R(e; V_1)] \\ &[L(\bar{e}; Z)L(\bar{e}; V_2) + R(\bar{e}; Z)R(\bar{e}; V_2)] \\ &[L(b; V_1)R(b; V_1)][L(b; V_2)R(b; V_2)]; \end{aligned} \quad (11)$$

and the kinematical functions

$$G_{322}(s_H; s; s_Z) = 2ss_Z(s + s_Z - 2s_H)L(s_H; s; s_Z) + 2; \quad (12)$$

$$G_{322}^a(s_H; s; s_Z) = s_H - 4ss_Z L(s_H; s; s_Z) + s_H - s - s_Z; \quad (13)$$

Further, a logarithm arises from the integration over the fermion propagator:

$$L(s_H; s_Z; s) = \frac{1}{P} \ln \frac{s_H - s_Z}{s_H + s_Z} \frac{s + P}{s} =: \quad (14)$$

All C- and G- functions are symmetrical in their last two arguments. The functions C_{233} and C_{223}^a get their dependences on m_b^2 both from the Higgs coupling to the b quarks and from the b quark trace.

The b-deers with light quarks have gluon exchange contributions. Their interference with the Higgs signal vanishes due to the color trace.

The remaining two types of interferences vanish,

$$H_e = H = 0: \quad (15)$$

In these two cases the b quark trace is odd in the b quark momenta: $\text{Tr}[(\not{p}_b + m_b)(\not{p}_b - m_b)(\not{v}_b + \not{a}_b) = 4m_b v_b(p_b - p_b)$; while the rest of the matrix element squared is independent of the b quark momenta. Since the angular phase space integration is symmetric in b and b as may be conveniently seen in the rest system of the bb system, the result of the integration is zero.

3 Results and discussion

The Higgs mass M_H is unknown. In the numerical examples it will be varied between 80 and 120 GeV. Within these bounds, the Higgs is extremely narrow; in the SM one expects $\Gamma_H < 10$ MeV. Figure 3 contains the total cross sections σ_T for the production of $b\bar{b}$, $(q\bar{q})b\bar{b}$, $(q\bar{q})$ as functions of the centre of mass energy \sqrt{s} from LEP 2 until NLC energies. The Higgs mass is assumed to be $M_H = 80$ and, for one of the curves, 120 GeV.

Figure 3: Total cross section $\sigma_T(e^+e^- \rightarrow f_1 f_1 f_2 f_2)$ in fb for several production channels as a function of \sqrt{s} . All (but one) curves are for $M_H = 80$ GeV and $\sqrt{s_Z}; \sqrt{s_H} > 60$ GeV. For the lower lying curve for $b\bar{b}$ production these values are set $M_H = 120$ GeV and $\sqrt{s_Z} > 60; \sqrt{s_H} > 100$ GeV; $q\bar{q} = uu + dd + ss + cc$.

Figure 4: The invariant mass distribution $\frac{d\sigma}{ds_H} = \frac{d\sigma}{ds_H} \frac{d\sigma}{ds_H}$ in fb/GeV for $b\bar{b}$ production as a function of the invariant Higgs mass $\sqrt{s_H}$ at $\sqrt{s} = 190$ GeV for $\sqrt{s_Z} > 60$ GeV and $M_H = 80$ GeV. The plus and minus signs indicate the sign of the interference between the Higgs signal and the background and the arrow at the resonance curve the peaking values of the module of the interference.

It is nicely seen that the gold-plated channel ($b\bar{b}$ production) is not that with the highest event rate. At the HZ production threshold (depending on the chosen Higgs masses at $\sqrt{s} = 171$ and 211 GeV) the cross sections rise steeply and fall then asymptotically like $1/s$. A round the threshold this behaviour would be spoiled by the photon exchange diagrams if there were not a cut $\sqrt{s_Z} > 60$ GeV. A stronger cut becomes possible only after the present Higgs mass limit of about 60 GeV from LEP 1 will be improved. Pure background (solid curve) has a similar though less pronounced behaviour with its threshold at 182 GeV. For $b\bar{b}$ production with $M_H = 120$ GeV the SM background is cut away by a dedicated cut on the background of $\sqrt{s_Z} > 100$ GeV. This cut will be allowed after a Higgs mass limit of 100 GeV will be established.

Figure 4 shows for $b\bar{b}$ production the invariant mass distribution $\frac{d\sigma}{ds_H}$ as a function of $\sqrt{s_H}$ at LEP 2 for $M_H = 80$ GeV. The extremely sharp Higgs peak ($M_H = 10^4$!) is more than four orders of magnitude above the background. The Higgs-background interference is extremely small, of the order of $M_H = 10^4$ compared to the signal and has a zero at the Higgs peak position. This justifies the general praxis to assume the Higgs production being on mass shell although only the decay products may be observed. The total cross section arises nearly exclusively from the Higgs peak region. Lower cuts may substantially reduce the background.

The cut on $\sqrt{s_Z}$ is of special theoretical interest. Figure 5 contains, for the $b\bar{b}$ channel, the invariant mass distribution $\frac{d\sigma}{ds_Z}$ as a function of $\sqrt{s_Z}$ at LEP 2 for $M_H = 80$ GeV. In fact, only the low energy region is shown. Non-negligible cross section contributions come from this region as may be seen from a comparison with figure 4 (compare the scales!). A cut on s_Z helps considerably to limit this noninteresting background. The origin are the photonic propagators in the on shell cross section, which cause a behaviour of the background proportional to $1/s_Z$. This becomes large if the invariant mass of the muon pair is as small as $\sqrt{s_Z} = 2m_\mu$.

Maybe here is the right place that one should mention all the interesting effects, which influence the various cross section parts and which from time to time become a point of discussion when

Figure 5: The invariant mass distribution $\frac{d\sigma}{ds_Z} = \frac{d\sigma}{ds_Z} \frac{ds_Z}{ds_Z}$ in fb/GeV for $b\bar{b}$ production as a function of the invariant Z mass $\sqrt{s_Z}$ for $\sqrt{s} = 190$ GeV and $\sqrt{s_H} > 60$ GeV.

different numerical results are compared. The following mass dependences are taken into account:

The m_b in the Higgs b quark coupling;

The m_b in the trace of the b-deer when interfering with the signal;

The m in the deers if no cut is applied to s_Z .

The first two items are evident from the formulae of section 2. The third one deserves a comment. The product $\frac{1}{(s_Z; m^2; m^2)} (1 + 2m^2/s_Z) D_B(s_Z) / s_Z$ contains, besides the propagator, a factor from phase space and one from the squared matrix elements. For extremely small s_Z , this combination yields for photon exchange ($B = \gamma$) a finite correction to the cross section of order $O(1)$ which is erroneously absent if the muon mass is set zero. (see figure 5, dashed line). Thus, in no-cut calculations this mass correction is not allowed to be left out while even a weak cut removes this dependence completely.

Further, we should mention that many other terms with a dependence on m_b^2 or m^2 also occur and could be also taken into account; not all of them are safely smaller than the Higgs-background interference. Since they are small and not of the leading order, we neglect them all.

A crude estimate of the peak position may be obtained for the on shell cross section by the following ansatz: $\frac{d\sigma}{ds_Z} \approx C \frac{s}{(M_Z + M_H)^2} s^{3/2}$. The extremum of this is located at $\sqrt{s_{\text{peak}}} = \frac{1}{3} (M_Z + M_H) \approx 1.22 (M_Z + M_H)$, which is a few dozens GeV away from the threshold and, of course, gets changed by a refined treatment and the more for the off shell case and with QED corrections. From figure 3 one may see that the peak position depends on the production channel so that a trivial universal estimation of $\sqrt{s_{\text{peak}}}$ seems not to exist. Finally, we also should mention that there are substantial radiative corrections to $4f$ production [1]. The discussion of them in [2] applies also here and the Fortran program 4fan, which was mentioned there has been used in order to produce the figures of this letter.

To summarize, we performed the first complete semi-analytical calculation of on mass shell SM Higgs production with background for the process $e^+e^- \rightarrow b\bar{b}$. The importance of the

various dependences on m_b and m_c has been studied. The Higgs background interferences either vanish identically after integration over the fermion angles or are extremely small due to the narrow Higgs width. The background may be reduced substantially by dedicated cuts on both virtualities s_H and s_Z . For practical purposes this means that Higgs model specialists may calculate their isolated Higgs signal contributions leaving out the background. The latter one may be added later incoherently while the Higgs background interferences may be safely neglected. These general conclusions apply also to physics beyond the SM as long as the Higgs width remains small.

References

- [1] J. Gunion, H. Haber, G. Kane and S. Dawson, *The Higgs Hunter's Guide*, (Addison-Wesley, Reading, 1990);
 P.M. Zerwas (ed.), *e^+e^- Colliders at 500 GeV: The Physics Potential*, Proceedings of the Munich-Annecy-Hamburg Workshop, 1991 (DESY Report 92{123A,B (1992)) and 1992 (DESY Report 93{123C});
 B. Kniehl, Phys. Repts. 240 (1994) 211; E. Gross, G. Wolf and B. Kniehl, Z. Physik C 63 (1994) 417.
- [2] D. Bardin, A. Leike and T. Riemann, Phys. Letters B 344 (1995) 383.
- [3] D. Bardin, A. Leike and T. Riemann, in: T. Riemann and J. Blumlein (eds.), *Proc. of the Zeuthen Workshop on Elementary Particle Theory { Physics at LEP 200 and Beyond*, Teupitz, Germany, April 1994, Nucl. Phys. B (Proc. Suppl.) 37B (1994) p. 274.
- [4] V. Barger, K. Cheung, A. Djouadi, B. Kniehl and P.M. Zerwas, Phys. Rev. D 49 (1994) 79;
 E. Boos, M. Sachwitz, H.J. Schreiber and S. Shichanin, Z. Physik C 61 (1994) 675;
 M. Dubinin, V. Edneral, Y. Kurihara and Y. Shimizu, Phys. Letters B 329 (1994) 379;
 F.A. Berends, R. Kleiss and R. Pittau, Nucl. Phys. B 424 (1994) 308; Nucl. Phys. B 426 (1994) 344; Leiden preprint INLO-PUB-12/94 (1994) [hep-ph/9409326], submitted to Comput. Phys. Commun.
- [5] J.A.M. Vermaseren, *Symbolic Manipulation with FORM* (CAN, Amsterdam, 1991);
 E. Boos et al., preprint KEK 92{47 (1992) and references therein.